Journal Name

COMMUNICATION

Novel fluorinated ligands for gold nanoparticle labelling with application in ^{19}F-MRI.

Received 00th January 20xx,
Accepted 00th January 20xx

DOI: 10.1039/x0xx00000x

www.rsc.org/

Olatz Michelena,[a] Daniel Padro,[a] Carolina Carrillo-Carrión,[a] Pablo del Pino,[b] Jorge Blanco,[a] Blanca Arnaiz,[a] Wolfgang J. Parak[a,c] and Mónica Carril*[a,d]

Novel fluorinated ligands for gold nanoparticle labelling have been designed and synthesised. Several types of gold nanoparticles have been prepared in the presence of these fluorinated ligands alone, or in combination with non-fluorinated ligands. Their colloidal stability in water and other solvents was tested and the magnetic resonance properties of the so-obtained nanoparticles was also assessed in detail. ^{1}H and ^{19}F-NMR spectra were evaluated and MRI phantoms of the most promising nanoparticles were succesfully measured in ^{19}F-MRI. The MRI signal to noise ratio was related to the fluorine concentration and compared with ICP-MS data to correlate the real concentration of fluorine grafted on the nanoparticles with the actually active fluorine in MRI.

Non-invasive imaging techniques are key tools in medicine for early detection and screening of severe pathologies, such as cancer or cardiovascular diseases. In particular, magnetic resonance imaging (MRI) is an interesting modality because of its good spatial resolution, average contrast agent sensitivity and lack of radiation risk. Fluorine 19 (^{19}F) based MRI is a re-emerging field with interesting features which complement proton-based MRI. Indeed, the applications of ^{19}F magnetic resonance are steadily growing in clinical and biomedical research.[1] The ^{19}F isotope has a 100% of natural abundance and its signal to noise ratio (SNR) in magnetic resonance is comparable to that of ^{1}H. The most interesting advantage of ^{19}F over ^{1}H is the negligible endogenous ^{19}F-MRI signal in the body, for which any detectable signal can only come from an exogenous probe. The highest concentration of fluorine is in the bones and teeth but since it is immobilised in a solid matrix its signal is undetectable. Unlike with currently in use probes in ^{1}H-MRI, the lack of background in ^{19}F-MRI images, and the fact that the probe is imaged directly, allow for the absolute quantification of the signal that is directly proportional to the probe concentration.[1] Furthermore, fluorine is commonly present in drugs for the treatment of numerous diseases[2] and their tracking by ^{19}F-MRI/MRS could be very useful to determine their pathways inside the body, as it was reported with 5-fluorouracil for the treatment of colorectal cancer.[3]

For all these reasons, ^{19}F-MRI has attracted the attention of many researchers, and the development of novel fluorine probes is a field of increasing interest. In particular, fluorine contrast agents are in the spotlight not only for their use as imaging probes, but also for their potential applications as activatable probes[4] and for cell tracking.[5] However, in order to achieve a quality of image similar to that obtained with ^{1}H-MRI, a high load of fluorine atoms is required. Perfluorocarbons (PFCs) are standard probes for ^{19}F-MRI because of their high content in fluorine, nonetheless only a few of those atoms have the same resonance frequency, which leads to chemical shift artefacts that complicate the image and cause a decrease in SNR.[1,6] Hence, a single overall resonance frequency is desirable and only achievable by the use of chemically equivalent fluorine atoms. To circumvent this limitation, some groups have used symmetrical dendrimers,[7] PEG polymers[8] or other probes such as perfluorinated crown ethers or hexafluorobenzene.[9]

The main challenge, however, when working with fluorinated compounds, is to overcome their intrinsic hydrophobicity to render them water soluble for biomedical applications, but at the same time keep a high local concentration of fluorine atoms for MR applications. So far, the main strategy is to encapsulate PFCs in emulsions of at least 200-300 nm, which limits their *in vivo* applications.[6] Some research groups have focused their attention on the synthesis of nanoparticles (NPs) decorated with fluorinated ligands to increase the local concentration of fluorine.[10] The group of Pasquato synthesised gold NPs coated with either thiolated PFCs modified with ethylenglycol moieties[11] or perfluorinated ethylenglycol

[a] CIC biomaGUNE, Paseo Miramon 182, 20009 Donostia - San Sebastian, Spain. E-mail: mcarril@cicbiomagune.es
[b] Centro Singular de Investigación en Química Biológica y Materiales Moleculares (CiQUS) y Departamento de Física de Partículas, Universidade de Santiago de Compostela, 15782, Spain.
[c] Department of Physics, Philipps University of Marburg, Renthof 7, 35037 Marburg, Germany.
[d] Ikerbasque, Basque Foundation for Science, 48011 Bilbao, Spain.

Electronic Supplementary Information (ESI) available: Ligand and NP synthetic procedures and characterization. NMR spectra of novel compounds. Histograms for all TEM images and further NP characterisation. Imaging methods description and materials and methods for cell viability assays. List of abbreviations. See DOI: 10.1039/x0xx00000x

derivatives.[12] In both examples they successfully overcame the hydrophobicity associated with fluorinated compounds and obtained water dispersible NPs. However, the use of non-equivalent fluorine atoms led to signal splitting or even quenching due to tight packing of the ligands. Taking this into account, synthetic modifications of fluorinated compounds remain yet to be conducted to achieve water dispersible gold NPs coated with ligands bearing chemically equivalent fluorine atoms.

In the present work, perfluorinated *tert*-butanol **1** was chosen as the virtually ideal fluorine reporter due to the great amount of equivalent fluorine atoms that have the same chemical shift and lack coupling with adjacent protons. In order to label gold NPs with these probes, a thiolated ligand was required. We proposed the synthesis of fluorinated thiol derivatives **2**-**4** shown in Figure 1 (See ESI for synthetic details). The use of ethylene glycol units in the linkers would firstly ensure the required flexibility and mobility of the fluorinated head, which is a key feature to be active in MR, and secondly they would enhance the hydrophilicity of the so-obtained NPs.

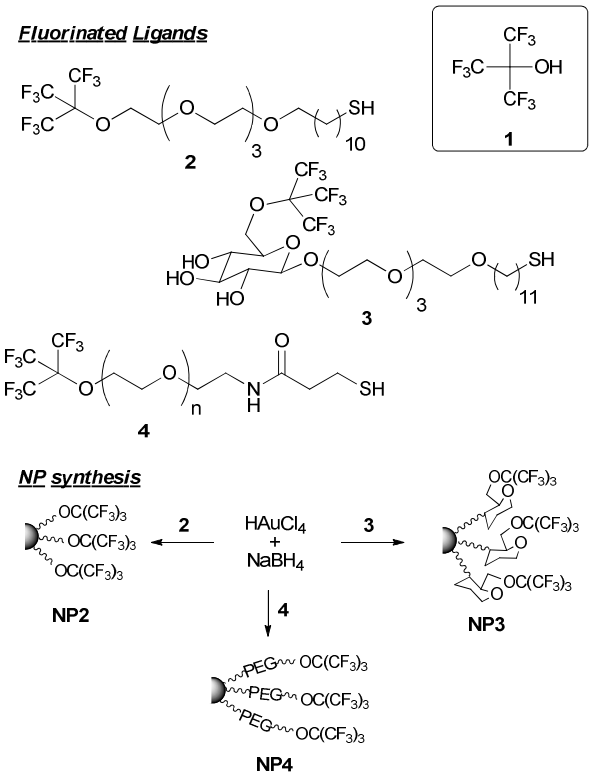

Figure 1. Fluorinated ligands prepared and the corresponding gold NPs obtained in their presence.

Fluorinated ligands **2**-**4** were successfully prepared and used to produce gold NPs via reduction of $HAuCl_4$ in the presence of $NaBH_4$ (See ESI). **NP2-4** of a core diameter ranging from approximately 2 to 4 nm were obtained by this method. After NP synthesis and prior to ^{19}F-NMR/MRI signal evaluation, it was crucial to make sure that all remaining unbound ligand was removed from the NP solution. This was confirmed by ^{1}H-NMR, by the complete disappearance of the signal corresponding to the methylene group adjacent to the thiol (δ ≈ 2.5 – 2.8 ppm), which was cancelled when the ligand was linked to the NP due to tight packing of ligands (Figure 2A *vs*. 2B). Indeed it was observed that for ligands **2**-**3** the NMR signal of the whole aliphatic chain was affected due to the self-assembly of ligands on the NP surface. In the case of **NP4**, the complete disappearance of both the methylene signal by the thiol (δ ≈ 2.8 ppm) and that by the carbonyl group (δ ≈ 2.5 ppm) was noticed (Figure 2B). ^{19}F-NMR spectra of both free ligands and NPs were also measured. As expected, only one peak for all 9 equivalent fluorine atoms was detected and the chemical shift of fluorine atoms when free or attached to gold did not vary significantly (δ = -71.48 ppm and -71.33 ppm for free ligands and NPs, respectively). The shape of the signal barely changed upon NP formation, suggesting that NPs are sufficiently homogeneous to keep all fluorine atoms environment similar and mobile enough not to broaden the NMR signal significantly (Figure 2C). In addition, the so-obtained NPs were characterised by UV-Vis absorption spectroscopy and transmission electron microscopy (TEM) analysis (Figure 2D-G and Figure S2 in ESI).

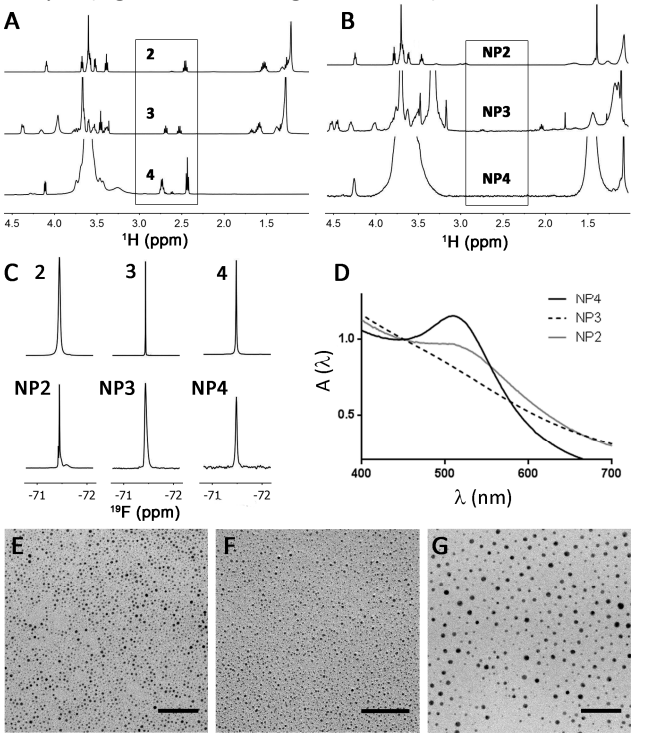

Figure 2. A). ^{1}H-NMR of free ligands **2-4** with a highlight on the $–CH_2$-S peaks position. B) ^{1}H-NMR of **NP2**-**4** with a highlight on the absence of $–CH_2$-S signal. C) ^{19}F-NMR spectra of **2**-**4** and **NP2**-**4**. D) UV-Vis spectra of **NP2** (in CH_2Cl_2), **NP3** (in MeOH) and **NP4** (in H_2O), normalised at λ = 450 nm. E-F) TEM micrographs of **NP2**-**4** (from left to right). Scale bars represent 50 nm. See ESI for TEM analysis.

The amount of **2**-**4** used to stabilise each NP ranged from 3 to 0.45 equivalents, which led to varied core sizes in the synthesis as shown by TEM and by the different size of the plasmon resonance band in UV-Vis spectra (Figure 2D-G). Next, the colloidal stability of the NPs was assessed and it was observed that **NP2** was stable in chlorinated solvents and ^{i}PrOH, but neither in shorter chain alcoholic solvents nor in water. **NP3** was neither stable in chlorinated solvents nor in water, but it could be dispersed in EtOH, MeOH and acetone. On the contrary, PEGylated **NP4** was colloidally stable in both

organic solvents and water. NPs remained unchanged after storage at 4 °C either dry or in solution for at least 6 months. It was observed in the synthesis of **NP4** that when a Au:**4** ratio of 1:0.2 was used, the NPs were successfully obtained and signal was detected in ^{19}F-NMR when measured in CD_2Cl_2. However, when exactly the same sample was measured in D_2O, the fluorine signal disappeared almost completely suggesting that the packing of **4** was not very tight, thereby giving the hydrophobic fluorine atoms the chance to hide within the PEG chains. On the contrary, when the ratio was increased from 0.2 to 0.45, little difference was observed between measuring the ^{19}F-NMR spectra of the same sample either in organic solvent or in water, suggesting that the increased number of PEG ligands led to a more packed structure which forced most of fluorine atoms to be exposed and active in MR (Figure S3 in ESI). In an attempt to make **NP2**-**3** water dispersible, part of fluorinated ligands **2**-**3** were replaced by ligands **5**-**7** functionalised with hydrophilic moieties (Figure 3). **NP2A-C** and **NP3A** were not colloidally stable in water when replacing 50 % or less of fluorinated ligand **2**-**3** by hydrophilic ligands. On the contrary, **NP3B** was colloidally stable in water with only 25 % of replaced ligands by **6**. The longer ethylenglycol moiety in **6** may be responsible for its greater water solubility (See ESI).

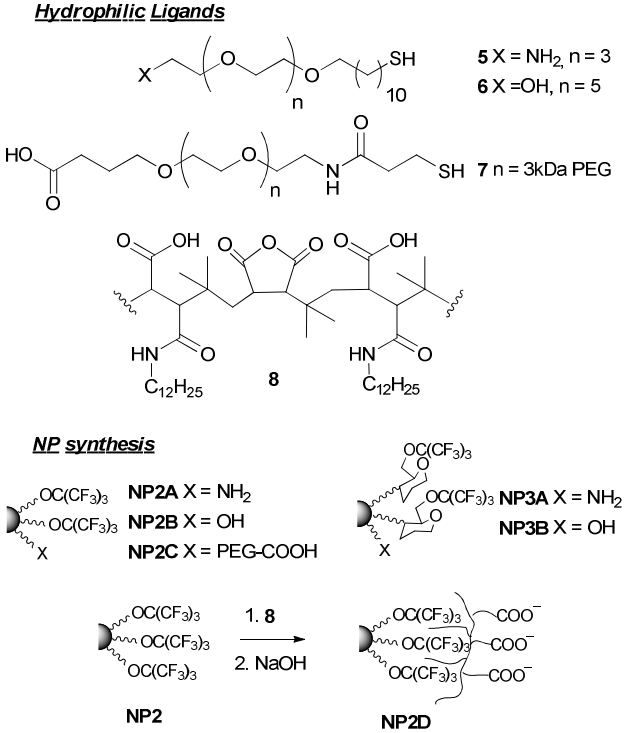

Figure 3. Structure of hydrophilic ligands **5**-**8**, **NP2B**-**D** and **NP3A**-**B**.

Lastly, we decided to coat **NP2** with water soluble polymer **8** derived from poly(isobutylene-alt-maleic anhydride) (PMA). Hence, commercially available PMA was reacted with dodecylamine as described before[13] and used for coating hydrophobic **NP2**, by intercalation of the dodecylamine chains in between the fluorinated ligands. After treatment with aqueous NaOH, all unreacted anhydride rings opened and transformed into carboxylate groups, rendering **NP2D** stable in water (See ESI). When small amounts of polymer were used, only partial coating was observed, and NPs were not well dispersed in water. On the contrary, by increasing the polymer amount per NP, full coating was obtained, but groups of NPs formed along with very few single NPs, as observed by TEM (Figure 4D).[14] In **NP2A**-**D** and **NP3A**-**B**, the ^{19}F-NMR signal split into 2 peaks or distributions, more or less overlapped depending on the NPs, which account for at least two different spatial distributions or environments around fluorine atoms due to the presence of two types of ligands (Figure 4A and FigureS1 in ESI). Encapsulation of **NP2** with **8** mostly quenched the ^{19}F-NMR signal due to lack of mobility of the fluorine atoms under the polymer coating (Figure 4A).

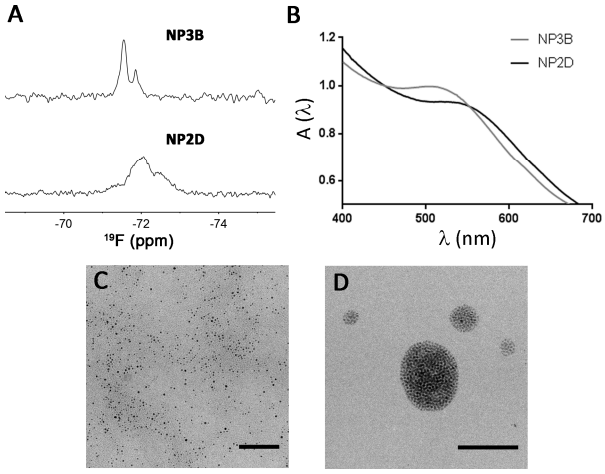

Figure 4. A) ^{19}F-NMR spectra of **NP3B** and **NP2D** recorded in a mixture of D_2O/H_2O. B) UV-Vis spectra of **NP3B** and **NP2D** recorded in water and normalised at λ = 450 nm. C-D) TEM micrographs of **NP3B** and **NP2D** (from left to right). Scale bars represent 100 nm.

Finally, phantoms were prepared to probe the potential use of the fluorinated ligands prepared herein as fluorine labels for MRI on gold NPs (See ESI for imaging protocols). Selected NPs were **NP2**, **NP4** and **NP2D**. In all cases, phantoms were acquired simultaneously with increasing amounts of the corresponding ligand **2** or **4** for SNR calibration. In the first experiment ligand **2** and **NP2**, both dissolved in CD_2Cl_2, were successfully imaged almost down to 3 mM concentration in fluorine (Figure 5A). In the second experiment ligand **4**, **NP4** and **NP2D** in water were analysed (Figure 5C). **NP4** was successfully imaged, but signal from **NP2D** was at the level of noise, as expected given the broad signal observed in ^{19}F-NMR after coating with **8**. As shown in Figure 5B and 5D, SNR of the ^{19}F-MRI signal of **2** and **4** was in linear relationship with the amount of fluorine atoms in solution. ICP-MS analysis of **NP2** and **NP4** showed that the gold content for each NP was 10.5 % and 40.7 % of the total mass analysed, respectively. These values were used to calculate fluorine concentration for each NP sample in Figure 5. Hence, by using the calibration data obtained from the ligand solutions and the SNR measured for each NP sample it was possible to study how much of the fluorine present on each type of NP was actually active in the MRI experiments performed. Surprisingly, it was observed that only 40 % of the fluorine on **NP2** was being imaged, whereas 80 % of the fluorine in **NP4** showed to be active in MRI. This raises the question on how fluorine is actually placed on the

NPs. For **NP4**, it may indicate that most of fluorine atoms are exposed on the surface and mobile. On the contrary, on **NP2** it seems that more than half of fluorine atoms are either hidden or packed too tightly to be detected. After successful imaging of **NP4** and given its water solubility, preliminary cell viability and apoptosis tests were performed in order to consider them for future *in vivo* applications. Hence, increasing concentrations of **NP4** (0 - 50 nM) were incubated with three different cell lines (MDA-MB-231, C33-A and MDA-MB-435S). MTS cytotoxicity assay showed that those cell lines were still viable after 24 hours of exposure (Figure 5E and Figure S6 in ESI). Likewise, the Annexin V apoptosis assay did not indicate apoptosis of cells after 24 hours of incubation with **NP4** for the cell lines tested (Figure 5F) (See ESI).

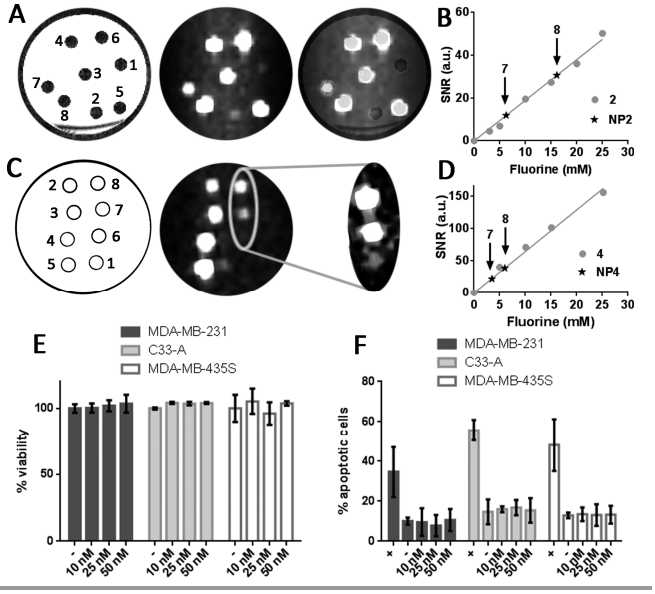

Figure 5. A) From left to right: ^{1}H-MRI; ^{19}F-MRI and ^{1}H-^{19}F overlay of **2** and **NP2**. Samples 1-6 contained **2**, 7-8 contained **NP2**. Concentration data are referred to fluorine: 1 = 3 mM; 2 = 5 mM; 3 = 10 mM; 4 = 15 mm; 5 = 20 mM; 6 = 25 mM; 7 = 16.8 mM; 8 = 33.6 mM. All samples were in CD_2Cl_2. B) Representation of SNR of fluorine signal with respect to fluorine concentration. C) From left to right: ^{1}H-MRI; ^{19}F-MRI and zoomed-in region of ^{19}F-MRI. Sample 1 contained water for physical reference, samples 2-5 contained **4**, 6 contained **NP2D** and 7-8 contain **NP4**. Concentration data are referred to fluorine: 2 = 5 mM; 3 = 10.1 mM; 4 = 15.1 mM; 5 = 25.2 mM; 6 = 8 mM; 7 = 4.2 mM; 8 = 8.3 mM. All samples were in water. D) Representation of SNR of fluorine signal with respect to fluorine concentration. E) MTS viability assay after 24 hours incubation of **NP4** with 3 different cell lines and at different NP concentrations (0-50 nM). F) Percentage of apoptotic cells of the same cell lines with **NP4**. A positive control was obtained after incubation with apoptosis inducer staurosporin (1 μM). A negative control was obtained after measuring apoptosis in cells in the absence of both **NP4** and staurosporin.

Hence, novel fluorinated ligands **2**-**4** have been designed, synthesised and used for the preparation of gold NPs functionalised with fluorine atoms. Several strategies have been tested to overcome the intrinsic hydrophobic nature of fluorinated compounds to finally obtain colloidally stable NPs in water, out of which the use of long chain PEGylated compounds has proved to be the best option. The so-obtained NPs have been characterised with regard to their ^{19}F-NMR and ^{19}F-MRI signal to test their potential use as contrast agents. These NPs represent an improvement with respect to currently in use probes, due to the single chemical shift and high local concentration of fluorine atoms, which could enhance SNR in imaging applications. In addition, preliminary viability assays performed with **NP4** indicate the possibility of exploring their use for *in vivo* studies by ^{19}F-MRI.

Acknowledgments. MC acknowledges Ikerbasque for a Research Fellow position. MINECO is acknowledged for funding through the call RETOS (CTQ2015-68413-R to MC). CCC acknowledges MINECO for a Juan de la Cierva—Incorporación contract. Marta Gallego is kindly thanked for some of the TEM micrographs. Javier Calvo is kindly thanked for the HRMS of novel compounds. Karsten Kantner is kindly thanked for ICP-MS analysis. Parts of this work were supported by the German Research Foundation (DFG grant PA 794/25-1 to WJP).

References

1 (a) J. Ruiz-Cabello, B.P. Barnett, P.A. Bottomley, J.W.M. Bulte, *NMR Biomed.*, 2011, **24**, 114; (b) I. Tirotta, V. Dichiarante, C. Pigliacelli, G. Cavallo, G. Terraneo, F.B. Bombelli, P. Metrangolo, G. Resnati, *Chem. Rev.*, 2015, **115**, 1106; (c) J. Chen, G.M. Lanza, S.A. Wickline, *WIREs Nanomed. Nanobiotechnol.*, 2010, **2**, 431.

2 (a) J. Wang, M. Sanchez-Rosello, J.L. Acena, C. del Pozo, A.E. Sorochinsky, S. Fustero, V.A. Soloshonok, H. Liu, *Chem. Rev.*, 2014, **114**, 2432; (b) S. Purser, P.R. Moore, S. Swallow, V. Gouverneur, *Chem. Soc. Rev*. 2008, **37**, 320; (c) K.L. Kirk, *J. Fluorine Chem.*, 2006, **127**, 1013.

3 D.J.O. McIntyre, F.A. Howe, C. Ladroue, F. Lofts, M. Stubbs, J.R. Griffiths. *Cancer Chemother. Pharmacol.,* 2011, **68**, 29.

4 (a) Y. Yuan, H. Sun, S. Ge, M. Wang, H. Zhao, L. Wang, L. An, J. Zhang, H. Zhang, B. Hu, J. Wang, G. Liang, *ACS Nano*, 2015, **9**, 761; (b) X. Huang, G. Huang, S. Zhang, K. Sagiyama, O. Togao, X. Ma, Y. Wang, Y. Li, T.C. Soesbe, B.D. Sumer, M. Takahashi, A.D. Sherry, J. Gao, *Angew. Chem. Int. Ed.*, 2013, **52**, 8074; (c) S. Mizukami, R. Takikawa, F. Sugihara, Y. Hori, H. Tochio, M. Wälchli, M. Shirakawa, K. Kikuchi, *J. Am. Chem. Soc.* 2008, **130**, 794.

5 (a) M. Srinivas, P. Boehm-Sturm, C.G. Figdor, I.J. de Vries, M. Hoehn, *Biomaterials*, 2012, **33**, 8830; (b) E.T. Ahrens, J. Zhong, *NMR Biomed*. 2013, **26**, 860; (c) E.T. Ahrens, R. Flores, H. Xu, P.A. Morel, *Nat. Biotechnol*., 2005, **23**, 983.

6 (a) C.C Jacoby, S. Temme, F. Mayenfels, N. Benoit, M.P. Krafft , R. Schubert, J. Schrader, U. Flögel, *NMR Biomed.*, 2014, **27**, 261; (b) M.M. Kaneda, S. Caruthers, G.M. Lanza, S. A. Wickline, *Ann. Biomed. Eng.*, 2009, **37**, 1922.

7 K.J. Thurecht, I. Blakey, H. Peng, O. Squires, S. Hsu, C. Alexander, A.K. Whittaker, *J. Am. Chem. Soc.,* 2010, **132**, 5336.

8 C. Biaggi, M. Benaglia, M. Ortenzi, E. Micotti, C. Perego, M.-G. De Simoni, *J. Fluorine Chem.*, 2013, **153**, 173.

9 L. Mignion, J. Magat, O. Schakman, E. Marbaix, B. Gallez, B.F. Jordan, *Magn. Reson. Med.* 2013, **69**, 248.

10 P. Pengo, L. Pasquato, *J. Fluorine Chem*., 2015, **177**, 2.

11 C. Gentilini, F. Evangelista, P. Rudolf, P. Franchi, M. Lucarini, L. Pasquato, *J. Am. Chem. Soc.*, 2008, **130**, 15678.

12 M. Boccalon, P. Franchi, M. Lucarini, J.J. Delgado, F. Sousa, F. Stellacci, I. Zucca, A. Scotti, R. Spreafico, P. Pengo, L. Pasquato, *Chem. Commun.*, 2013, **49**, 8794

13 A.J. Lin, R.A. Sperling, J.K. Li, T.Y. Yang, P.Y. Li, M. Zanella, W.H. Chang, W.J. Parak, *Small*, 2008, **4**, 334.

14 This might be a consequence of the particular non-covalent interactions that organofluorine is able to establish, such as F-F interactions, which may bring NPs together at high concentration and promote the coating in groups rather than individually. See: (a) I. Alkorta, J. Elguero, *Struct. Chem*., 2004, **15**, 117; (b) D. O'Hagan, *Chem. Soc. Rev*. 2008, **37**, 308.

